Phase-stability study of the Al-Nb system

C. Colinet and A. Pasturel
Laboratoire de Physique Numérique des Systèmes Complexes (CNRS), Maison des Magistères, CNRS B.P. 166, 38042 Grenoble, France

D. Nguyen Manh and D. G. Pettifor
Materials Modelling Laboratory, Department of Materials, University of Oxford, OX1 3PH Oxford, United Kingdom

P. Miodownik
Department of Materials Science and Engineering, University of Surrey, Surrey GU2 5XH, United Kingdom
(Received 9 December 1996; revised manuscript received 24 March 1997)

The total energies of formation of Al-Nb intermetallic phases Nb_3Al ($A15$), Nb_2Al (σ), and $NbAl_3$ (DO_{22}) have been calculated using the linear-muffin-tin-orbital (LMTO) method in the full potential (FP) approach. Relaxation and distortion effects have been included and have been shown to play an important role in the stabilization of the DO_{22} intermetallic phase. In order to get the interaction parameters to describe the energetics of the bcc and fcc solid solutions, FP-LMTO calculations have been performed for various superstructures based on the bcc and fcc lattices. To discuss thermodynamic properties and the phase diagram of the Al-Nb system, the cluster variation method configurational entropy has been introduced using the tetrahedron-octahedron approximation in the fcc solid solution and the tetrahedron approximation in the bcc solid solution. The thermodynamic data obtained in this work agree fairly well with the available experimental data. Connections with Calphad approaches are also discussed. An attempt to calculate composition-temperature phase diagram of the Al-Nb system is presented, using a semiempirical treatment of the liquid phase. [S0163-1829(97)04826-1]

I. INTRODUCTION

The modern theory of phase diagram calculations has been made possible by great advances in band-structure calculations and theories of configurational thermodynamics and phase transformations. Total energy calculations based on the local density approximation (LDA) are now sufficiently accurate to explain many properties of materials in terms of the underlying electronic structure.[1] An accurate calculation of the configurational free energy of the alloy is possible within various approximations such as mean-field methods [cluster variation method[2] (CVM)] or by numerical methods (Monte Carlo simulations[3]). In these models, it is assumed that the internal energy can be written as a sum of multisite interactions which converge rapidly. The fact that these interactions can be derived from first-principles calculations establishes the basis of a comprehensive first-principles theory of cohesive, structural, and thermodynamical properties of metals and alloys. Two extreme types of approach to the calculation of these interactions have been developed.

(i) The first one starts from the energy of the completely disordered solid solution calculated by the coherent potential approximation[4] (CPA). The effective cluster interactions are calculated by the generalized perturbation method (GPM) of Ducastelle and Gautier,[5] the concentration waves theory of Gyorffy and Stocks,[6] and the embedded cluster method of Gonis *et al.*[7] using a perturbative treatment about the completely disordered state. In this case, the ordering energies can be written as an expression in terms of concentration-dependent nth-order effective cluster interactions. The GPM can be developed with the first-principles multiple-scattering formalism of the Korringa-Kohn-Rostoker coherent-potential approximation or with the first-principles tight-binding linear muffin-tin coherent-potential approximation. For instance, such approaches have been used to study the thermodynamics of surface alloys.[8]

(ii) In the second approach a limited set of periodic structures representative for a given problem is chosen and their total energies are calculated using first-principles self-consistent calculations. It was suggested by Connolly and Williams[9] that the effective cluster interactions can be obtained from these total energies. The method was developed further by Zunger and co-workers[10] and is called the renormalized interaction approach. Standard *ab initio* band-structure techniques applied to suitable chosen small supercells can be used, and the double-counting terms are included. On the other hand, as the interaction energies, which are of order of a few mRy, are obtained as differences of total energies, the numerical requirements are severe. This procedure has been used successfully by several authors[11–18] and will be adopted in the present work.

The Al-Nb system presents both theoretical and technological interest, the aluminides like TiAl or Nb_3Al having many desirable properties such as low density, high melting temperature, and high yield strength. However, their well-known brittleness at ambient temperatures must be overcome. One strategy for circumventing this brittle behavior is to use a combination of rapid solidification processing and ternary alloying to induce the $B2$ structure which results in alloys that are significantly more ductile. Unfortunately, this phase often transforms to a metastable ω phase which may drastically embrittle these $B2$ phases of transition metal aluminides. Therefore Nguyen-Manh *et al.*[19] have recently stud-

ied the relative stability at $T=0$ K of the ω phase with respect to the other close-packed hcp, fcc, and bcc phases. Indeed, of primary importance in attempting to engineer the properties of the Al-Nb alloys is an understanding of the equilibrium and metastable phases in the system and their range of stability and metastability with respect to experimentally controlled parameters such as composition and temperature. However, in spite of the extensive amount carried out so far in this system, thermodynamic research has been limited to few investigations.[20,21] An assessment of the experimental work which has been performed to study the equilibrium in this system can be found in Ref. 22. This assessed diagram is characterized by the occurrence of three intermediate phases: Al_3Nb, which melts congruently near 1953 K and whose structure is a fcc closed-packed superlattice DO_{22};[23] $AlNb_2$, which melts peritectically near 2213 K and which has a σ structure; and $AlNb_3$, which decomposes peritectically near 2333 K and has an $A15$ Laves phase structure.[23] The Al_3Nb compound has a narrow range of stability around the stochiometric composition, while the two other compounds show relatively large domains of existence. The solubility of aluminum in solid bcc niobium extends to 20% at the peritectic temperature of the Nb_3Al compound. There is no major disagreement concerning this phase diagram. However, Menon *et al.*[24] report on a slightly lower solubility of aluminum in solid niobium.

In this paper we present preliminary results of a theoretical study of the composition temperature phase diagram in the Al-Nb system. In such a study, the relative stability of the three occurring Al_3Nb, Nb_2Al, and Nb_3Al compounds has to be understood. Their formation energies are calculated using the full-potential (FP) linear muffin-tin-orbital (LMTO) method in order to analyze the physical origin of their stability at $T=0$ K. The total energies of selected superstructures based on fcc and bcc lattices are calculated using the same method. These *ab initio* calculations not only confirm the instability of fcc Nb at 0 K under a tetragonal Bain distortion,[25] but show that this instability extends at least until 0.75 Nb composition. Concerning bcc solid solutions, the *ab initio* calculations also show that the $B2$ structure for NbAl is unstable with respect to tetragonal distortion; namely, for the ideal ratio $c/a=1$, the curvature of the energy versus c/a is negative, corresponding to a maximum of the energy; these results are in agreement with those presented by Asta *et al.*[26] Two sets of effective cluster interactions (ECI's) are then derived for bcc- and fcc-based disordered alloy phases using the renormalized interaction approach. These ECI's will be used in conjunction with the CVM to determine the necessary thermodynamic properties as a function of composition and temperature for bcc and fcc solid solutions. More particularly, we focus our attention on the lattice stability of niobium, namely, the differences of Gibbs energies of fcc Nb and bcc Nb. The vibrational effects are also included in these calculations using the Debye-Grüneisen model, but these effects appear very small compared with the chemical effects. A comparison with the CALPHAD analyses is proposed. An attempt to calculate the Al-Nb phase diagram also needs a knowledge of the thermodynamic properties of the liquid phase. We propose an estimation of the chemical mixing energy and of the first-neighbor pair interactions to deal with the short-range order in this phase. The calculation of these first-neighbor pair interactions has been based on the results obtained in both the bcc and fcc solid solutions. Various approximations are used for the modeling of the Gibbs energy of the liquid phase: a subregular model, a quasichemical model, and an estimation of the ordering energy from the one deduced in a fcc solid solution using a CVM treatment in the regular tetrahedron approximation. The influence of these various liquid-phase models on the phase diagram is discussed. The lattice stability of aluminum can be taken from either the *ab initio* calculations or from CALPHAD compilations; the latter values lead to a slight increase in the aluminum solubility in bcc niobium.

The remainder of the paper is organized as follows: In Secs. II and III the details of the electronic structure calculations and the method of obtaining the ECI's are presented. In Sec. IV, the thermodynamic data of the solid solutions will be calculated and we will discuss the lattice stability of fcc Nb with respect to bcc Nb. In Sec. V, we will also propose various modeling for the liquid phase. In Sec. VI, a complete Al-Nb equilibrium phase diagram is calculated using estimations of the entropies of formation of the intermetallic compounds and the influence of the aluminum lattice stability on the solubility of aluminum in bcc niobium will be presented.

II. TOTAL-ENERGY CALCULATIONS

As a first step, we have studied the relative stability of the three intermediate phases observed in the equilibrium phase diagram. In Structurbericht notation, these phases are called DO_{22} (Al_3Nb) phase, σ phase ($AlNb_2$), and $A15$ phase ($AlNb_3$).[23] We have also calculated the total energies of selected superstructures: $A2$, DO_3, $L6_0$, $B2$, $B32$, $A1$, and $B11$ based on a bcc and $A1$, $L1_2$, DO_{22}, $L1_0$ based on a fcc lattice. Our purpose in performing total-energy calculations of Al-Nb bcc and fcc superstructures is to obtain a set of effective cluster interactions which can be used to study phase stability and the effect of composition and the state of order on the properties of the solid solutions in this alloy system. For this reason, the number of superstructures for which these total-energy calculations must be performed is equal or greater than the number of effective cluster interactions which is expected to be important for describing the energetics of this system. In particular, the stability of a DO_{22} relative to an $L1_2$ structure, such as is experimentally observed for the 0.75 composition in aluminum in this system, can only be modeled by a set of effective cluster interactions which includes interaction parameters beyond the range of the first-nearest-neighbor pair of the fcc lattice. Furthermore, the effect of structural relaxation on the total energy of all the fcc and bcc superstructures must be taken into account since these energies are to be used for the purpose of studying the relative stability of various alloy phases in this system. In previous studies concerning the aluminum-titanium system,[15] Asta *et al.* have shown that the tetragonal distortion of DO_{22} must be taken into account to predict that the DO_{22} structure is more stable than the $L1_2$ structure for Al_3Ti composition. We must, therefore, find the minimum of the total energy with respect to all structural degrees of freedom for all the ordered compounds, including those which

TABLE I. Calculated energies of formation referred to bcc Nb and fcc Al of some face-centered-cubic Nb-Al superstructures. In column 7 are reported the values obtained when relaxation effects lead to a minimization of the total energy.

Composition	Strukturbericht	Pearson symbol	Space group	Prototype	$\Delta_f H$ (kJ/mol of atoms)	$\Delta_f H$ relaxed and distorted (kJ/mol of atoms)
Al	$A1$	$cF4$	$Fm3m$	Cu	0	
Al_3Nb	$L1_2$	$cP4$	$Pm3m$	Cu_3Au	−25.3	
Al_3Nb	$D0_{22}$	$tI8$	$I4/mmm$	$TiAl_3$	−32.1	−41.5
AlNb	$L1_0$	$tP4$	$P4/mmm$	CuAu	−26.1	
$AlNb_3$	$L1_2$	$cP4$	$Pm3m$	Cu_3Au	−10.1	
$AlNb_3$	DO_{22}	$tI8$	$I4/mmm$	$TiAl_3$	−3.2	
Nb	$A1$	$cF4$	$Fm3m$	Cu	33.1	

are not experimentally observed. For instance, the total energies of NbAl in the $B33$ (CrB-type), $B19$ (hcp-like), and ω structure[19] have been also calculated to compare the relative stability of various NbAl structures and to understand why no intermetallic compound is stable for the equiatomic composition.

A. Computational details

To calculate the energies of the different phases quoted above, we employ the all-electron total-energy local density formalism as carried out with the linear muffin-tin-orbital (LMTO) method in the full potential (FP) approximation.[27,28] In this approach, the linear muffin-tin orbitals are augmented with numerical solutions of the radial Schrödinger equation within nonoverlapping muffin-tin spheres. No spherical shape approximation for the potential or charge density is made; in the interstitial region, these quantities are expressed in Hankel-function expansions as proposed by Methfessel.[29]

The LMTO basis includes s, p, and d functions for each atom. For the full-potential calculations, it is necessary to extend the basis using LMTO's with various localizations. The niobium aluminides valence states are of predominant Nb $(4d)$ and Al $(3sp)$ character, and in the present calculations we have used as the basis function 22 atom-centered augmented Hankel functions per Al and 29 per Nb sites. The corresponding decay energies in the Hankel function tails are $-K^2=-0.01$ (spd for Al or $spdf$ for Nb), $-1{,}0$ (spd), and -2.3 Ry (sp). In order to make accurate predictions we have also included a second ''semicore'' panel to provide bandlike treatment of both the Nb $4s$ and $4p$ states. To evaluate integrals over the Brillouin zone, we use a uniform mesh of sampling points which ensure that the total energy is converged to within 0.1 mRy per atom. The charge density is calculated exactly in the muffin-tin spheres in angular momentum up to $l=4$. We use the same angular momentum cutoff in the interpolation of quantities in the interstitial region, expanded in Hankel functions of energies -1 and -3 Ry.[30] All LDA results reported in this paper are scalar relativistic calculations using the exchange-correlation potential of von Barth and Hedin.[31]

For each phase, the total energies provided by the LMTO method are obtained for different values of the volume; the minimum of this curve determines the equilibrium total energy and the equilibrium volume. The bulk modulus which is related to the curvature of the total energy with volume is obtained using a fit based on Murnaghan's equation of state.[32] Since the total energies of the pure metals are treated in the same way, the formation energy is obtained by subtracting the weighted sum of total energies of the constituent elements from the total energy of the compound, namely,

$$\Delta_f E = E - x_{\mathrm{Al}} E_{\mathrm{Al}} - x_{\mathrm{Nb}} E_{\mathrm{Nb}}.$$

It should be noted that the ground states of Al and Nb are predicted to be fcc and bcc, respectively. The energy differences between the fcc and bcc structures, defined as $E_i^{\mathrm{fcc}} - E_i^{\mathrm{bcc}}$, are -8.1 and 33.1 kJ/mol for Al and Nb, respectively. At high temperature in the Nb-rich part, the Al-Nb phase diagram can be viewed as resulting from a competition between the bcc solid solution and two intermetallic compounds. In the Al-rich part, the very great stability of the DO_{22}, Al_3Nb phase must be understood. Therefore it seems to be important to compare the stability of the three intermetallic compounds, namely, $A15$, σ, and DO_{22} structures with superstructures occurring on the fcc and bcc lattices, in addition to obtaining the ECI's in the disordered bcc and fcc solid solutions.

B. Phase stability of superstructures based on a fcc lattice

The fcc superstructures considered in this study are displayed in Table I. The space-group symmetry given in Table I dictates the degrees of freedom for structural relaxation. The fcc $A1$ and $L1_2$ have cubic symmetries, and the only degree of freedom is the lattice parameter a. DO_{22} is body-centred tetragonal while $L1_0$ is tetragonal; in these structures, the lattice parameters a and c need to be varied independently in the total-energy calculations. When uniform changes of volume are the only structural relaxations of periodic Al-Nb structures, the values of the energies of formation at equilibrium referred to fcc Al and bcc Nb are reported in column 6 of Table I. The values of the formation energies referred to fcc Al and fcc Nb are plotted versus Al composition in Fig. 1.

The calculated molar volumes of the structures considered in this study are plotted in Fig. 2 as function of Al composition. A significant deviation from Vegard's law (dashed line) is observed. The deviation is maximum at 75 at. % Al. The same behavior was observed by Asta *et al.*[15] for the fcc

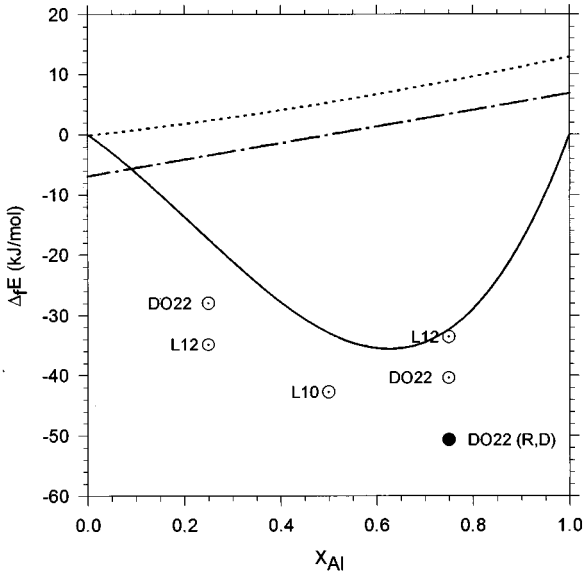

FIG. 1. Energies of formation of Nb-Al fcc superstructures: ⊙, unrelaxed structures: ●, relaxed structures (Sec. II); disordering energy (solid line), first-nearest-neighbor pair interaction (dashed line), and second-nearest-neighbor pair interaction (Sec. V) (dot-dashed line).

Ti-Al intermetallic compounds. Figure 3 shows the dependence of the calculated bulk moduli on the aluminum composition.

Changes in the total energy caused by deviations of c/a ratios and interatomic distances from their ideal values considerably affects the value of the enthalpy of formation of the DO_{22} superstructure for the 75% Al composition. The value of the ratio c/a which minimizes the total energy is 2.227,

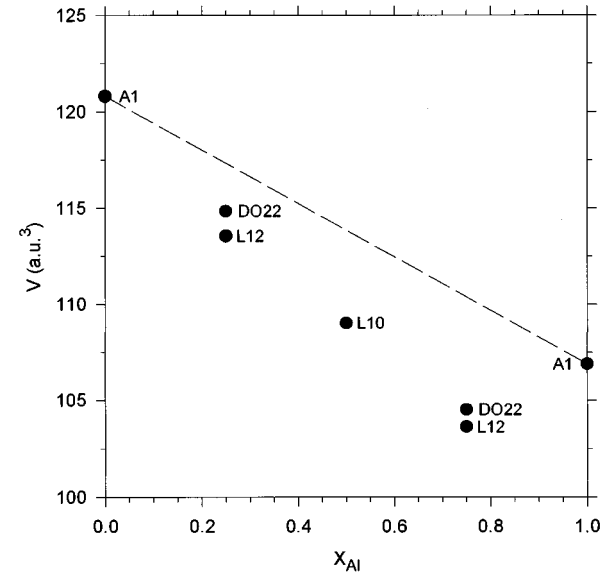

FIG. 2. Calculated molar volumes of fcc Nb-Al intermetallic compounds vs Al composition for the five fcc superstructures considered in this study. The dashed line indicates the dependence of the molar volume on composition expected from Vegard's law.

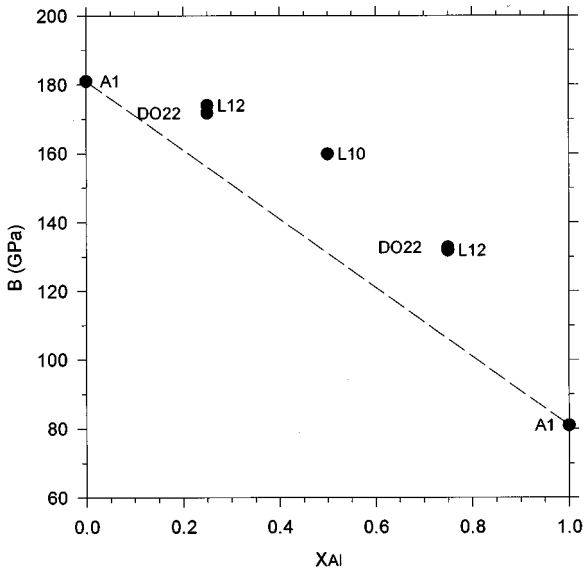

FIG. 3. Calculated bulk moduli of fcc Nb-Al intermetallic compounds vs Al composition for the five fcc superstructures considered in this study.

while the experimental value reported in the *Pearson's Handbook* is 2.232. The value of the enthalpy of formation of the relaxed and distorted DO_{22} phase is reported in the last column of Table I and in Fig. 1. The effect of the c/a relaxation in the case of the $L1_0$ structure is rather small and has been neglected.

Recent *ab initio* calculations[25] suggest that fcc Nb is mechanically unstable with respect to tetragonal distortions. Therefore we have performed calculations of elastic constants of fcc Nb, and our calculations confirm that the elastic constant C of fcc Nb is negative, which implies a dynamical instability with respect to tetragonal distortion. Similar calculations show that $L1_2$ and DO_{22} structures for the Nb_3Al stochiometry are also mechanically unstable: however, for the AlNb $L1_0$ compound, the coefficient C' becomes positive, and therefore this compound is mechanically stable with respect to tetragonal distortion.

C. Phase stability of superstructures based on a bcc lattice

The bcc superstructures considered in this study are displayed in Table II. When uniform changes of volume are the only structural relaxations of periodic Al-Nb structures, the values of the energies of formation referred to bcc Al and bcc Nb are displayed in Fig. 4 as function of Al composition. The calculated volumes and bulk moduli are displayed, respectively, in Figs. 5 and 6, which show similar features to the fcc superstructures.

Changes in the total energy caused by deviations of c/a ratios and interatomic distances from their ideal values considerably affect the value of the enthalpy of formation of the $L6_0$ superstructure at 25% and 75% of aluminum, and of the $A1$ and $B11$ superstructures for equiatomic composition. The values of the energies of formation referred to fcc Al and bcc Nb are reported in Table II.

Both Asta *et al.*[26] and Nguyen-Manh *et al.*[19] have pointed out that the AlNb $B2$ structure was unstable with respect to

TABLE II. Calculated energies of formation referred to bcc Nb and fcc Al of some centered-cubic Nb-Al superstructures. In column 7 are reported the values obtained when relaxation effects lead to a minimization of the total energy.

Composition	Strukturbericht	Pearson symbol	Space group	Protype	$\Delta_f H$ (kJ/mol of atoms)	$\Delta_f H$ relaxed and distorted (kJ/mol of atoms)
Al	$A2$	$cI2$	$Im3m$	W	8.1	
Al_3Nb	DO_3	$cF16$	$Fm3m$	BiF_3	15.3	
Al_3Nb	$L6_0$	$tP4$	$P4/mmm$	$CuTi_3$	−6.7	−25.0
AlNb	$B2$	$cP2$	$Pm3m$	CsCl	−0.4	
AlNb	B32	$cF16$	$Fd3m$	NaTl	−6.8	
AlNb	$B11$	$tP4$	$P4/nmm$	γ-TiCu	−2.4	−14.3
AlNb	$A1$	$oC8$	$Cmmm$	γ-IrV	−19.0	−29.3
$AlNb_3$	DO_3	$cF16$	$Fm3m$	BiF_3	−6.1	
$AlNb_3$	$L6_0$	$tP4$	$P4/mmm$	$CuTi_3$	−9.4	−16.1
Nb	$A2$	$cI2$	$Im3m$	W	0	

tetragonal distortion. Furthermore, Asta *et al.*[26] have presented the evolution of the energy of formation as function of the c/a ratio and found that the lowest energy for the NbAl compound with $B2$ order is obtained for a value of c/a roughly equal to 1.45, which is close to the value when the distorted $B2$ is equivalent to an ideal $L1_0$ structure. In the present work, we found that the c/a relaxation in the case of the $L1_0$ structure was rather small. The difference of the total energies of the $B2$ and $L1_0$ structures calculated in this work is of the same order of magnitude as the one shown in a graph by Asta *et al.*[26] For the $B32$ phase we found a value of C' near zero at the ideal ratio $c/a=1$ in agreement with the result proposed by Asta *et al.*[26] These authors found a second minimum for a ratio c/a roughly equal to 1.58. However, the energy of formation at this second minimum is more positive than the one obtained for the $B2$ distorted structure.

Asta *et al.*[26] proposed that the so-called $B2$ in quenched Nb-rich alloys is not strictly cubic, but that the crystallographic data supports the idea that it has undergone a partial Bain transformation. However, the calculations performed by Nguyen-Manh *et al.*[19] show that the ω phase is more stable than either $L1_0$ and $L1_2$ (see Fig. 7) and suggest an alternative explanation, supported by evidence from Passa *et al.*,[33] that the structure of such quenched $B2$ alloys is related to the ω phase.

D. Phase stability of $AlNb_2(\sigma)$ and $AlNb_3(A15)$ compounds

In a previous work dealing with the metastability of the ω phase in transition-metal aluminides, Nguyen-Manh *et al.*[19]

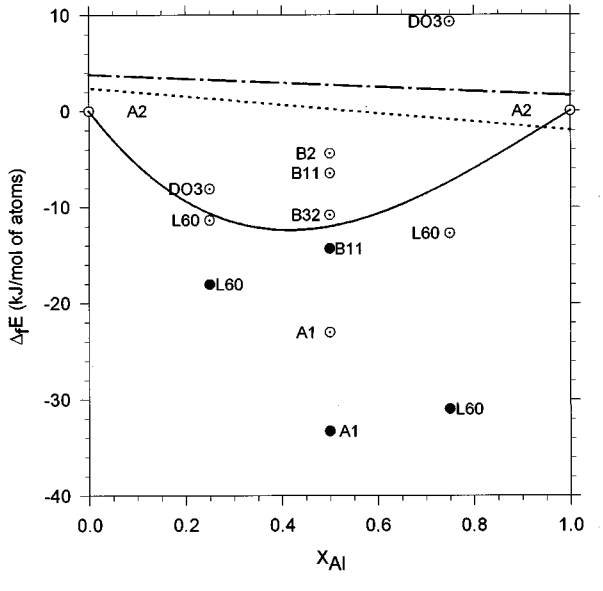

FIG. 4. Energies of formation of Nb-Al bcc superstructures: ⊙, unrelaxed structures: ●, relaxed structures (Sec. II); disordering energy (solid line), first-nearest-neighbor pair interaction (dashed line), and second-nearest-neighbor pair interaction (Sec. V) (dot-dashed line).

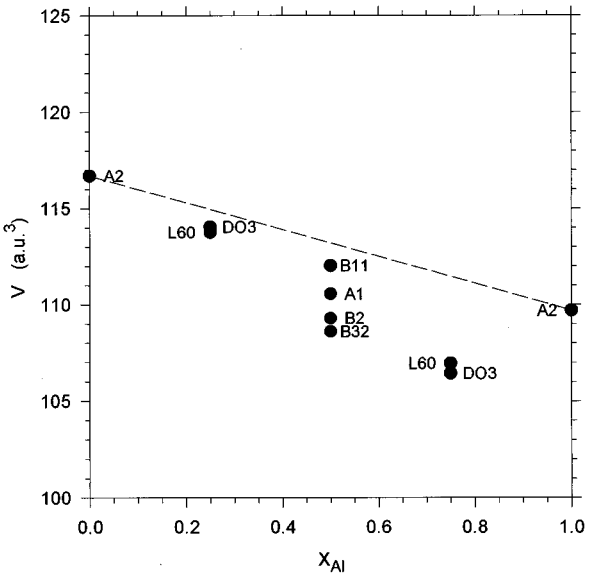

FIG. 5. Calculated molar volumes of bcc Nb-Al intermetallic compounds vs Al composition for the eight bcc superstructures considered in this study. The dashed line indicates the dependence of the molar volume on composition expected from Vegard's law.

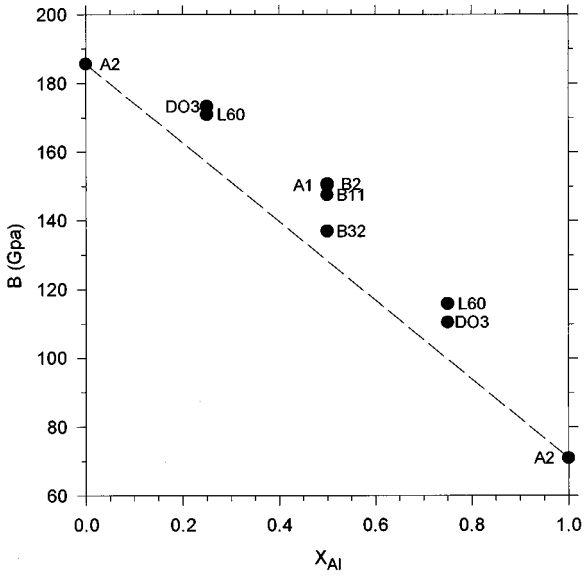

FIG. 6. Calculated bulk moduli of bcc Nb-Al intermetallic compounds vs Al composition for the eight bcc superstructures considered in this study.

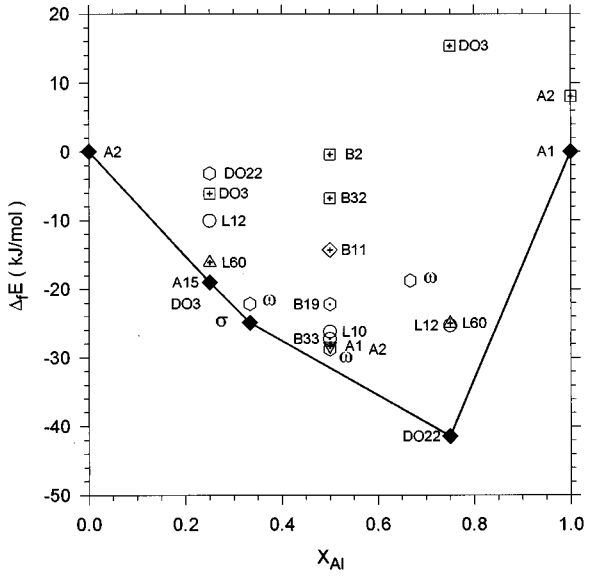

FIG. 7. Calculated energies of formation of perfectly ordered NbAl intermetallic compounds. The reference state is bcc Nb and fcc Al.

calculated with the FP-LMTO method the total energies of the compounds $AlNb_3$ ($A15$ structure), $AlNb_2$ (σ structure), Al_3Nb (DO_{22} structure), $AlNb_2$, AlNb, and Al_2Nb in the omega (ω) structure, and AlNb in the $B19$ structure (hcp-like) and $B33$ structure (NaCl prototype). Only the main conclusions of this previous work are reported here. The values of the energies of formation reported by these authors and those obtained in this work for the bcc and fcc structures are reported in Fig. 7. (Note that in the case of relaxation effects only the values of the energies of the corresponding state have been reported). In agreement with the experimental phase diagram, Al_3Nb in DO_{22} structure, $AlNb_2$ in σ structure, and $AlNb_3$ in $A15$ structure are found to be the ground state. By comparing the stability with other AB competing phases, the ω phase in Al-Nb was found to be the most metastable phase for the 0.5 composition. However, as shown in Fig. 7, the combination of nearby stoichiometries Al_3Nb and $AlNb_2$ cause AlNb to be metastable.

The energies of formation at $T=0$ K of $AlNb_3$ ($A15$ structure), $AlNb_2$ (σ structure), and Al_3Nb (DO_{22} structure) compounds referred to fcc Al and bcc Nb are reported in Table III where they are compared with experimental values of the enthalpies of formation at room temperature. Using direct calorimetric measurements, Meschel and Kleppa[20] derived the enthalpies of formation at room temperature of two compounds: $AlNb_3$ and Al_3Nb. For the first compound the value obtained by these authors is less exothermic than the calculated value, but for the Al_3Nb compound the agreement between the experimental and calculated values is very satisfactory. Values of the enthalpies of formation of the niobium aluminides were also proposed by Shilo *et al.*[21] These authors used a Knudsen effusion method, and so the values of the enthalpies of formation are not obtained directly. Using the second and third laws Shilo *et al.*[21] derived the values of the enthalpies of formation of the three intermetallic compounds at 298 K, and these values are reported in Table III. The agreement between the calculated values and experimental one seems acceptable.

III. CLUSTER EXPANSIONS AND EFFECTIVE CLUSTER INTERACTIONS

A. Cluster expansion

As discussed in the Introduction, the study of the evolution of the structural stability as a function of composition

TABLE III. Comparison of the calculated energies of formation of $AlNb_3$ ($A15$), $AlNb_2$ (σ), and Al_3Nb (DO_{22}) compounds and the experimental values obtained by Meschel and Kleppa (Ref. 20) and Shilo *et al.* (Ref. 21).

Enthalpies of formation (kJ/mol of atoms)	Calculated values This work	Experimental values Meschel and Kleppa[a]	Experimental values Shilo *et al.*[b]
$AlNb_3$	−19.0	−13.7	−19.3
$AlNb_2$	−24.9		−25.0
Al_3Nb	−41.5	−40.5	−32.6

[a]Reference 20.
[b]Reference 21.

TABLE IV. Effective cluster interactions for fcc-based Nb-Al alloys. The point correlation function is related to the molar fractions of Al and Nb by the relation $\xi = x_{\mathrm{Nb}} - x_{\mathrm{Al}}$. The reference state of the energy is fcc Al and fcc Nb.

Symbol	Coordinates	Multiplicity $m\alpha$	$m\alpha\ E\alpha$ (kJ)
$E(0,1)$		1	−32.9
$E(1,1)$	(0 0 0)	1	19.9
$E(2,1)$	(0 0 0), (1/2 0 1/2)	6	31.9
$E(2,2)$	(0 0 0), (1 0 0)	3	−0.1
$E(3,1)$	(0 0 0), (1/2 1/2 0), (1/2 0 1/2)	8	0.7
$E(3,2)$	(0 0 0), (1/2 0 1/2), (1 0 0)	12	−20.6
$E(4,1)$	(0 0 0), (1/2 0 1/2), (1/2 1/2 0), (0 1/2 1/2)	2	1.1

and temperature requires the definition of the parameters used in the three-dimensional (3D) Ising model. We use the renormalized interaction approach[9,10,16] assuming that the total energy of a A_xB_{1-x} compounds based on a same lattice can be described in terms of a rapidly convergent series of composition-independent multisite interactions. More precisely, we assume that the total energy of a particular configuration α is expressed by

$$E^{\alpha}_{\mathrm{tot}}(r) = \sum_{\gamma}^{\gamma_{\max}} N_{\gamma} E_{\gamma}(r) \xi^{\alpha}_{\gamma}. \tag{1}$$

$E_{\gamma}(r)$ is the composition-independent multisite interaction associated with the multisite correlation function ξ^{α}_{γ} defined in a given structure α as

$$\xi^{\alpha}_{\gamma} = \frac{1}{N_{\gamma}} \sum_{|n_j|} \sigma^{\alpha}_{n_1} \sigma^{\alpha}_{n_2} \sigma^{\alpha}_{n_3},$$

where $\sigma_n = 1 - 2p_n$ takes the value $+1$ or -1 depending on the occupancy of site n, N_{γ} is the total number of γ-type clusters, and the sum runs over all γ-type clusters that can be formed by combining sites on the entire crystal. From a finite number of total energies for ordered structures and by truncating the summation of Eq. (1), a set of multisite interactions is obtained from

$$E_{\gamma}(r) = \frac{1}{N_{\gamma}} \sum_{\alpha} [\xi^{\alpha}_{\gamma}]^{-1} E^{\alpha}_{\mathrm{tot}}(r) \quad \text{for } \phi < \gamma < \gamma_{\max},$$

$$E_{\gamma}(r) = 0 \quad \text{for } \gamma_{\max} < \gamma < \infty.$$

ϕ is the empty cluster.

Since $E^{\alpha}_{\mathrm{tot}}(r)$ is generally a function of volume, the interactions $E_{\gamma}(r)$ depend on r too. For a given $\gamma_{\max}$, the best set of cluster interactions has been chosen as the one which minimizes the predictive error in the energy according to

$$\sum_{\alpha} \omega_{\alpha} \left[E^{\alpha}_{\mathrm{tot}}(r) - \sum N_{\gamma} E_{\gamma}(r) \xi^{\alpha}_{\gamma} \right]^2 = \min, \tag{2}$$

with the weights $\omega_{\alpha} = 48 N_c(\alpha)/N_G(\alpha)$. Here $N_c(\alpha)$ and $N_G(\alpha)$ are the number of atoms per unit cell and the number of point group operations for the structure α, respectively. Formula (2) was suggested by Lu *et al.*[16] We find that different choices of weighting factor marginally affect the extracted ECI's, and therefore we take $\omega_{\alpha} = 1$. The optimum set of ECI's is then obtained by studying the convergence of the predictive error involved in the predicting energy values and also the convergence of the formation energy of the random alloy at 50%. This later one is also a significant check as it is obtained as a by-product in the used method.[15]

The volume dependence of the ECI's is implicitly included when they are determined with the inversion scheme using the values of the functions of configuration at the volumes for which the energy of the alloy is minimized at 0 K. In the particular case of the Al-Nb alloy, all the assumptions used to derive ECI's have only very weak consequences since the domain of the bcc solid solution is small and the fcc solid solution does not appear in the phase diagram.

B. Effective cluster interactions in the fcc lattice

The set of structures can be chosen in such a way to determine the chemical interactions parameters for all clusters up to the regular nearest-neighbor tetrahedron cluster in the fcc lattice. Within this approximation we need only the values of the pure fcc metals energies and three values of ordered compounds energies including AlNb in the $L1_0$ structure, and Al_3Nb and $AlNb_3$ on the $L1_2$ structure. However, the results obtained in Sec. II show that the DO_{22} superstructure is more stable than the $L1_2$ superstructure for 0.25 Al composition as well for the 0.75 Al composition. Then the second-nearest-neighbor pair interactions have to be taken into account in the set of ECI's.

Since the energy of formation is asymmetric with respect to 0.5 composition, it is expected that interactions of clusters containing an odd number of sites have to be included to reproduce it. Then a set of seven interactions has been chosen and evidently reproduces the energies of formation of the seven structures considered in this work. This set of clusters consists of the empty and point clusters, the nearest- and next-nearest-neighbor pairs, $E(2,1)$ and $E(2,2)$, the two first three-point clusters: the equilateral triangle $E(3,1)$, containing three first-nearest-neighbor pair interactions, and the isosceles triangle $E(3,2)$, containing two first-nearest-neighbor pair interactions and one second-nearest-neighbor pair interaction, and the nearest-neighbor regular tetrahedron $E(4,1)$. The set of ECI's included in the fit is given in Table IV. The value of $E(3,1)$ is very small because the energies of formation of the $L1_2$ superstructures for 0.25 and 0.75 aluminum composition have quite the same values (when referred to fcc Al and Nb). The value of $E(3,2)$ is much larger

TABLE V. Effective cluster interactions for bcc-based Nb-Al alloys. The point correlation function is related to the molar fractions of Al and Nb by the relation $\xi = x_{\mathrm{Nb}} - x_{\mathrm{Al}}$. The reference state of the energy is bcc Al and bcc Nb.

Symbol	Coordinates	Multiplicity $m\alpha$	$m\alpha\ E\alpha$ (kJ)
$E(0,1)$		1	−13.1
$E(1,1)$	(0 0 0)	1	−5.1
$E(2,1)$	(0 0 0), (1/2 1/2 1/2)	4	2.4
$E(2,2)$	(0 0 0), (1 0 0)	3	9.6
$E(2,3)$	(0 0 0), (1 0 1)	6	10.0
$E(2,5)$	(0 0 0), (1 1 1)	12	−5.6
$E(3,1)$	(0 0 0), (1/2 1/2 1/2), (1 0 0)	12	2.6
$E(3,2)$	(0 0 0), (1/2 1/2 1/2), (1 0 1)	12	−3.6
$E(3,3)$	(0 0 0), (1/1 1/2 1/2), (1 1 1)	4	6.1
$E(4,1)$	(0 0 0), (1/2 1/2 1/2), (1/2 1/2 −1/2), (1 0 0)	6	−3.3

because of the asymmetrical shape with respect to 0.5 composition of the energies of formation of the DO_{22} superstructures for 0.25 and 0.75 Al composition.

In order to test the convergence of this set of seven interactions, we have first reduced the number of interactions. For a set of six interactions, namely, without the regular tetrahedron, the total energies of ordered structures are reproduced with a root-mean-square error of 1 mRy/atom. Then we can consider that the chosen interactions capture the major effects to explain the structural stabilities of these structures. Another test is to compare the formation energies of compounds determined by the cluster expansion with the formation energies determined by a direct calculation for structures which do not enter the building of this set, namely, the $MoPt_2$ and ''40'' structures. We have found an energy difference of less than 1 mRy/atom for all the three considered structures.

C. Effective cluster interactions in the bcc lattice

In the bcc lattice the set of structures may be chosen in such a way as to determine the chemical interaction parameters for all clusters up to the irregular tetrahedron. Within this approximation we need only the values of the pure bcc metals and the four values of ordered compound energies including AlNb in the $B2$ and $B32$ structures, and Al_3Nb and $AlNb_3$ in the DO_3 structure. However, the results obtained in Sec. II show that the $L6_0$, $A1$, and $B11$ superstructures are more stable than the DO_3, $B2$, and $B32$ superstructures at the corresponding composition; then, third- to fifth-neighbor pair interactions have to be included to obtain a good fit of the energies of the bcc superstructures. However, as considered in other work,[16] we did not include the fourth-neighbor pair interaction since this one is outside the cube. Due to the importance of the third- and fifth-neighbor pair interactions, triangles containing these pairs have been considered in the set of ECI's to obtain a good convergence of the cluster expansion (1). More, when the first four-site cluster (the irregular tetrahedron including four first-nearest-neighbor pairs and two second-next-nearest pairs) is introduced, the fit of the compound energies is improved with rather small changes of the formation energy of the random alloy and of the pair and triangle interactions. The set of ECI's included in the fit is given in Table V.

Let us mention that the asymmetry around $c = 0.5$ is less pronounced than in the fcc lattice as indicated by the value of the triplet interaction. But what may be the most important feature is the different behavior between fcc-based pair interactions and bcc-based ones. The two nearest-neighbor pair interactions display the same positive sign, but an order of magnitude exists between both values. Then it is expected that the chemical ordering effects will not be quantitatively the same on the two lattices contrary to other systems like Ni-Al and Ni-Ti systems.[11,12]

IV. THERMODYNAMICS OF THE fcc AND bcc SOLID SOLUTIONS: LATTICE STABILITY OF NIOBIUM

A. Contributions to the Gibbs energy of mixing

The Gibbs energy of mixing of a phase α is defined as

$$\Delta_{\mathrm{mix}} G^{\alpha} = G^{\alpha} - x_A G_A^{\alpha} - x_B G_B^{\alpha},$$

where G^{α} is the Gibbs energy of the considered phase of structure α and G_i^{α} ($i = A$ or B) the Gibbs energy of pure i in the same structure α. In the Gibbs energy of mixing are included many terms: the configurational enthalpy of mixing, the configurational entropy of mixing, the relaxation energy, the electronic free energy of mixing, and the vibrational free energy of mixing. Note that in the following we will not distinguish the Gibbs energy of mixing from the free energy of mixing (as well as the enthalpy of mixing and the energy of mixing) because the difference equal to $P\ \Delta V$ is negligible except at very high pressure.

1. Configurational enthalpy of mixing

For the configurational enthalpy (or energy) of mixing, we will use the results obtained in Sec. III: The energy of mixing of the phase is expressed as a function of the cluster interactions.

2. Configurational entropy of mixing

The two solid solutions based on the bcc and fcc lattices are described as short-range-ordered solutions using the cluster variation method (CVM) in the tetrahedron approximation for the bcc lattice and the tetrahedron-octahedron approximation for the fcc lattice.

3. Relaxation energy

The origin of the relaxation energy has been explained in Sec. II in the case of perfectly ordered compounds and the corresponding energies have been calculated. This phenomenon may also occur in disordered phases; however, in this work we have not considered this effect because the bcc solid solution is stable in a small range of composition and the relaxation effects should be small. As the fcc solid solution does not appear in the phase diagram, we have not considered the relaxation effect in the fcc solid solution. However, the results obtained in the fcc solid solution can be related to the CALPHAD (Ref. 34) treatment of the lattice stability of niobium (see Sec. IV B).

4. Electronic free energy of mixing

It is possible to derive the electronic free energy by using the relation

$$F_{\mathrm{el}}(\sigma,T)=-\frac{\pi^2}{6}k_B^2T^2n_F(\sigma),$$

which is commonly referred to as the Sommerfeld model (to lowest order in temperature) for electron excitations. $n_F(\sigma)$ is the configurationally dependent density of state at the Fermi level at $T=0$ K. In the present work the thermodynamic data calculations will be performed at high temperatures around 2000 K. However, the electronic free energy of mixing, which is obtained by a difference between the electronic free energy of the disordered alloy and the pure elements in the same structure, is found to be an order of magnitude smaller than the configurational free energy, indicating that the electronic excitations give rise to negligible contributions to thermodynamic properties for Al-Nb system.

5. Vibrational free energy of mixing

The vibrational free energy of a phase is treated using the Debye model as generally formulated.[35] This needs the knowledge of the Debye temperature of the alloy and of the pure elements in the same structure. The Debye temperature can be defined in terms of a Debye sound velocity (C_D) by

$$\Theta_D=\frac{h^2}{2\pi k_B}\left(\frac{6\pi^2N}{V}\right)^{1/2}C_D.$$

Following Moruzzi *et al.*,[36] we will write C_D as a function of the equilibrium volume per atom and of the bulk modulus, data obtained from the *ab initio* calculations performed in Sec. II. However, it is impossible to apply this procedure for an unstable phase because at least one of their elastic constants is negative. Applying this scheme only to the stable and metastable phases, we have found, like for other systems, that the vibrational states primarily affect thermodynamic properties through their contribution to the entropy of Al-Nb alloys; however, the maximum value displayed by the vibrational free energy is found to be -2 kJ/atom, which is still to be an order of magnitude smaller than the configurational free energy at the same temperature, i.e., -50 kJ/atom for the fcc-based one.

B. fcc solid solution

1. Basic treatment

In the fcc solid solution the configurational entropy has been written in the tetrahedron-octahedron CVM approximation. This treatment allows us to take into account all the effective cluster interactions displayed in Table IV. The grand potential is minimized with respect to all correlation functions corresponding to clusters included in the tetrahedron and in the octahedron. The Newton-Raphson procedure is used to solve the minimization equations at fixed temperature and effective chemical potential. Then the enthalpy, entropy, and Gibbs energy of mixing can be computed as function of composition at constant temperature. The variations of the thermodynamic data of mixing at $T=2000$ K are displayed in Fig. 8 as function of Al composition. These results could be compared with those obtained using the CVM in the tetrahedron approximation assuming that the correlation functions of the clusters {2,2} and {3,2}, respectively, the second-next-neighbor pair and the second triangle, are given by $\xi_2^{(2)}=\xi_1^2$ and $\xi_3^{(2)}=2\xi_2^{(1)}\xi_1-\xi_1^3$, where ξ_1 is the point correlation function. The modification of the thermodynamic data of mixing resulting of the improvement of the entropy approximation is maximum in the domain of composition around $x_{\mathrm{Al}}=0.30$ (the molar enthalpy of mixing is about 5 kJ more negative, and the molar Gibbs energy of mixing is about 2.5 kJ more negative too); in the Al-rich domain, the differences are much smaller.

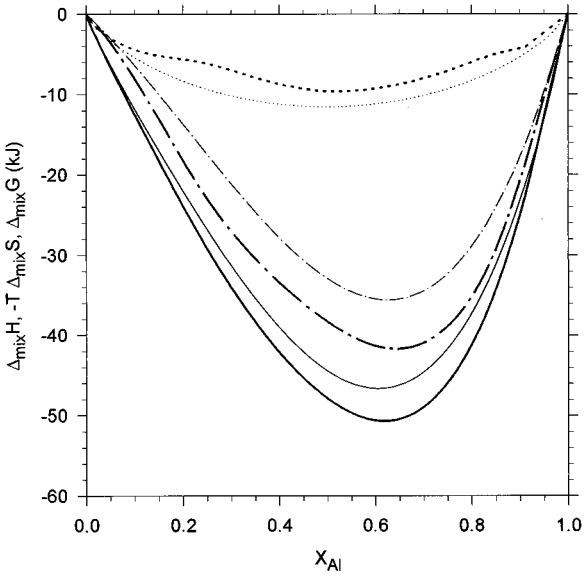

FIG. 8. Thermodynamic data of mixing in the fcc solid solution at $T=2000$ K. Thick lines: Gibbs energy of mixing (solid line), enthalpy of mixing (dot-dashed line), and $-T\Delta_{\mathrm{mix}}S$, where $\Delta_{\mathrm{mix}}S$ is the entropy of mixing (dashed line). Thin lines: same thermodynamic data without taking into account ordering effects.

The Gibbs energy of the fcc solid solution with the reference state bcc Nb and fcc Al is

$$G^{\mathrm{fcc}}=\Delta_{\mathrm{mix}}G^{\mathrm{fcc}}+x_{\mathrm{Nb}}(G_{\mathrm{Nb}}^{\mathrm{fcc}}-G_{\mathrm{Nb}}^{\mathrm{bcc}})^{\mathrm{LMTO}}. \tag{3}$$

The values of G^{fcc} are presented in Fig. 9. In Eq. (3) the difference $(G_{\mathrm{Nb}}^{\mathrm{fcc}}-G_{\mathrm{Nb}}^{\mathrm{bcc}})^{\mathrm{LMTO}}$ has been taken from the FP-LMTO calculations and is equal to 33.1 kJ/mol. The equivalent value for Nb used in thermodynamic databases such as presented by Saunders *et al.*[34] and by Fernandez-Guillermet and Huang[37] tend to be much lower and an explanation will be attempted. Following the approach of Fernandez-Guillermet[13] for W, the CALPHAD values generally derive from the extrapolation of experimental data in the region where the phase in question is stable, but in the case of Nb-Al, relevant solubility is far too small. It is, however, possible to apply the same extrapolative technique to that region of the calculated values in Fig. 9, which is far away from the region where the fcc phase has been shown to be mechanically unstable.

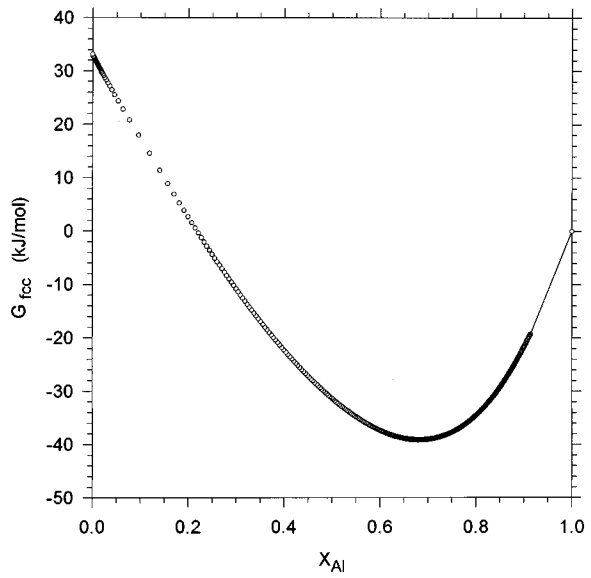

FIG. 9. Gibbs energy of formation of the fcc solid solution referred to bcc Nb and fcc Al: ●, estimated stable domain: ○ estimated unstable domain.

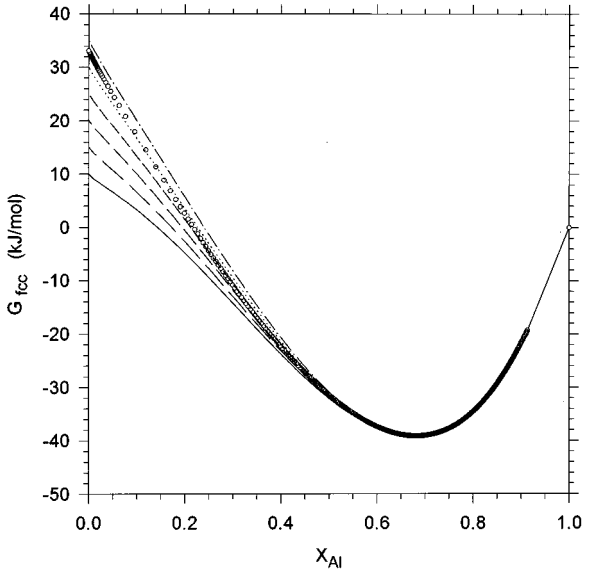

FIG. 10. Results of the fit of Eq. (6). The values of C_{Nb} stand between 10 and 35 kJ/mol.

2. Derivation of equivalent CALPHAD value

If we consider the values displayed in Fig. 9 as ''experimental values'' in the composition range where the fcc phase is stable, let us say when $0.6<x_{\mathrm{Al}}<1$, it is possible to extract the lattice stability for Nb bcc→fcc as derived in a CALPHAD treatment (following the method proposed by Fernandez-Guillermet *et al.*[13] to treat the lattice stability of W). The Gibbs energy per mol of atoms of the Al-Nb fcc solid solution referred to bcc Nb and fcc Al is then described by a substitutional solution model:

$$G^{\mathrm{fcc}}=x_{\mathrm{Nb}}(G^{\mathrm{fcc}}_{\mathrm{Nb}}-G^{\mathrm{bcc}}_{\mathrm{Nb}})^{\mathrm{CALPHAD}}+RT(x_{\mathrm{Al}}\ln x_{\mathrm{Al}}+x_{\mathrm{Nb}}\ln x_{\mathrm{Nb}})+{}^{E}G^{\mathrm{fcc}}, \tag{4}$$

where the sum of the last two terms corresponds to $\Delta_{\mathrm{mix}}G^{\mathrm{fcc}}$ in Eq. (3) with ${}^{E}G^{\mathrm{fcc}}$ being the nonideal term. In this work we will use a subregular solution approximation as in most CALPHAD calculations to express the excess Gibbs energy of mixing:

$${}^{E}G^{\mathrm{fcc}}=x_{\mathrm{Nb}}x_{\mathrm{Al}}[{}^{0}L^{\mathrm{fcc}}-{}^{1}L^{\mathrm{fcc}}(x_{\mathrm{Al}}-x_{\mathrm{Nb}})]. \tag{5}$$

The first term on the right side of Eq. (3) will be referred to a ''lattice stability'' in accordance with the CALPHAD convention and is written as

$$(G^{\mathrm{fcc}}_{\mathrm{Nb}}-G^{\mathrm{bcc}}_{\mathrm{Nb}})^{\mathrm{CALPHAD}}=A_{\mathrm{Nb}}-B_{\mathrm{Nb}}T. \tag{6}$$

The constants A_{Nb} and B_{Nb} represent the enthalpy and entropy differences between the nonstable and stable forms of niobium. In the following, we use a constant temperature $T=2000$ K. The term $A_{\mathrm{Nb}}-B_{\mathrm{Nb}}T$ is then constant and can be set equal to C_{Nb}.

In a series of fits of Eq. (4) as a function of the alloy composition, C_{Nb} has been chosen to vary systematically between 10 and 35 kJ/mol. That means that the function

$$Z=\frac{{}^{E}G^{\mathrm{fcc}}}{x_{\mathrm{Nb}}x_{\mathrm{Al}}}$$

has been fitted by a linear regression as function of $(x_{\mathrm{Al}}-x_{\mathrm{Nb}})$. Figure 10 shows the results of these fits for various values of C_{Nb}. A good fit of G^{fcc} values is obtained when C_{Nb} is about 20 kJ, which is of the same order of magnitude as bcc→fcc Gibbs energy differences for Nb obtained in CALPHAD-type analyses.[34,37,38]

C. bcc solid solution

In the bcc solid solution the basic cluster is an irregular tetrahedron which contains four pairs of first-nearest neighbors and two pairs of second-nearest neighbors. In this approximation the higher-order pair correlations (third- and fifth-nearest-neighbor pair interactions) will be treated in the mean-field approximation. To obtain the thermodynamic data of mixing at fixed temperature and composition, the Gibbs energy of mixing is minimized with respect to the tetrahedron probabilities. The enthalpy, entropy, and Gibbs energy of mixing at $T=2000$ K are displayed in Fig. 11 as function of Al composition. As a comparison, the curves obtained for these functions without taking into account the ordering effects have been drawn in this figure. The differences appear to be small; this observation is in agreement with the fact that the temperature is high and that the first- and second-neighbor pair interactions are small.

V. THERMODYNAMICS OF THE LIQUID PHASE

Liquid alloys may also display short-range order (SRO) as has been shown for a series of metallic alloys (see Ref. 12, for instance), and then it is essential to consider SRO when determining the thermodynamic data. The starting point to derive effective pair interactions for the liquid phase is the Carlsson's resummation procedure,[39,40] which corresponds to a high-temperature expansion of the correlation functions.

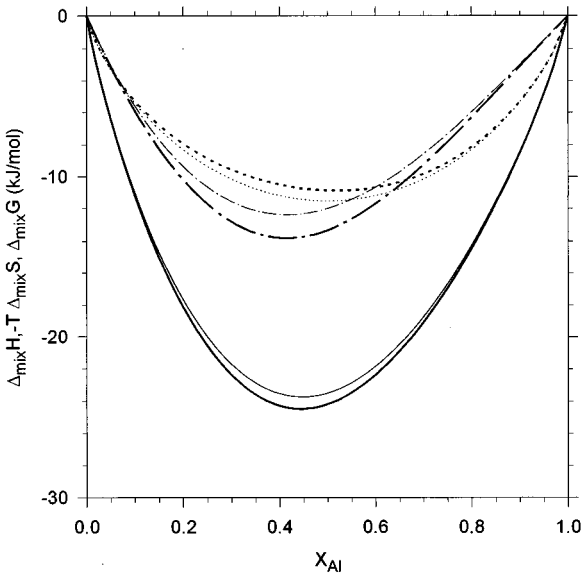

FIG. 11. Thermodynamic data of mixing in the bcc solid solution at $T=2000$ K. Thick lines: Gibbs energy of mixing (solid line), enthalpy of mixing (dot-dashed line), and $-T\Delta_{\mathrm{mix}}S$, where $\Delta_{\mathrm{mix}}S$ is the entropy of mixing. Thin lines: same thermodynamic data without taking into account ordering effects.

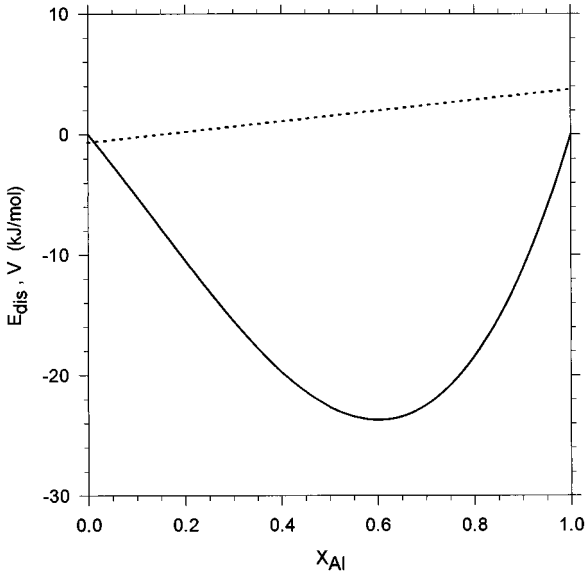

FIG. 12. Modeling of the liquid phase: disordering enthalpy of mixing (solid line) and first-nearest-neighbor pair interactions (dashed line).

Although this model is developed with a solid-state approximation, it does a good job of describing the influence of SRO on the thermodynamic properties of the liquids as seen for NiAl and NiTi alloys.[11,12] In these two systems we used the results obtained for the fcc solid solution, the disordering energy and the first-next-neighbor pair interactions, to model the thermodynamic data of mixing of the liquid phase. This choice is not critical in these systems as the disordering energy and the effective pair interactions display the same behavior in the fcc and bcc phases (see, for example, Figs. 4 of Ref. 12). However, in the case of the Nb-Al system, we observe that the disordering energies of the bcc and fcc solid solutions differ considerably (see Figs. 1 and 4). The disordering energy of the bcc phase is less negative than in the fcc phase: moreover, the disordering energy in the fcc phase presents a strong asymmetrical shape with respect to 0.5 composition. If we consider the Al-Nb-assessed phase diagram (see Ref. 22), it is clear that the liquid phase behaves similarly to the bcc phase in the niobium-rich range of composition, but behaves more like the fcc phase around the 0.75 Al composition (if one consider the large negative value of the enthalpy of formation of the Al_3Nb compound and the relatively low melting temperature of this compound). For these reasons we have chosen to model the disordering energy of the liquid phase in Nb-Al from the mean value of the disordering energy of mixing in the fcc and bcc phases. Similarly, the first-next-neighbor pair interactions used to describe the short-range order in the liquid phase were obtained from a mean value of the effective pair interactions obtained in the fcc and bcc phases taking into account the first- and second-next-nearest-neighbor pair interactions (their evolutions as a function of the composition are displayed in Figs. 1 and 4, respectively). The modeling of the liquid is presented in Fig. 12: Both the disordering energy and the first-next-nearest-neighbor pair interaction are plotted as function of Al composition. The thermodynamic data of mixing of the liquid phase have been calculated using various approximations: In the first one we did not consider the short-range order introduced by the effective pair interactions, and the liquid phase was treated as a subregular solution. In the second approximation a quasichemical model with a coordination number of 12 was used. In the third approximation the ordering energy and entropy were those obtained in a fcc solid solution using the regular tetrahedron as basic cluster, as done in previous works.[11,12] The Gibbs energies of mixing of the liquid phase obtained with these various approximations are displayed in Fig. 13. The differences are very small for two reasons: The temperature is high and the value of the effective pair interaction is small. Unfortunately, there are no experimental data in the Nb-Al liquid phase which will allow the models to be distinguished. In the following phase diagram calculations, the third approximation has been adopted. The thermodynamic data of mixing of the liquid phase at $T=2000$ K are presented in Fig. 14.

VI. PHASE DIAGRAM CALCULATIONS

Let us sum up the strategy of our calculations.

(i) The bcc solid solution in the niobium-rich part of the phase diagram is described as a short-range-ordered solution using the CVM tetrahedron approximation.

(ii) The liquid phase is described as a short-range-ordered phase for which the CVM in the regular tetrahedron approximation has been applied.

(iii) The three compounds occurring in the phase diagram are considered as stoichiometric compounds. Their enthalpies of formation referred to bcc Nb and fcc Al have been obtained from the FP-LMTO calculations.

However, the following data cannot as yet be obtained from first principles and have to be estimated.

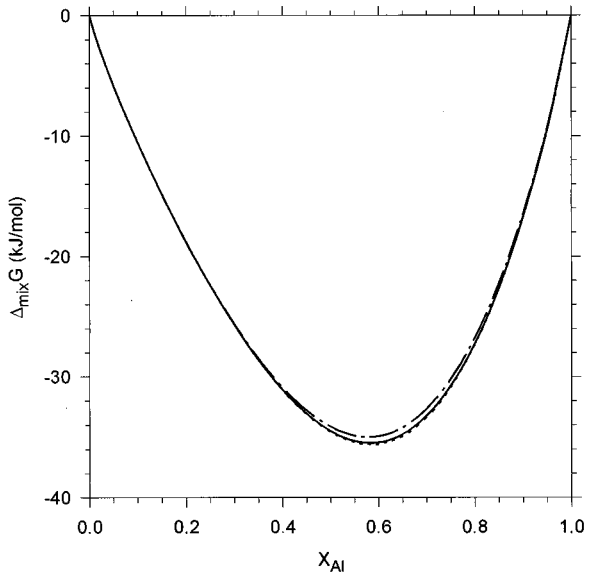

FIG. 13. Gibbs energy of mixing of the liquid phase at $T=2000$ K: subregular model (dot-dashed line) quasichemical model (dashed line), and CVM model (see text, Sec. 5) (solid line).

(i) Although the density functional theory has made significant progress in the modeling of liquids, application to the determination of the melting temperature and of the melting enthalpy still does not appear possible. Therefore we have chosen to use assessed thermodynamic data[38] which give the Gibbs energy of fusion for Al and Nb using the simple formulation

$$\Delta_{\mathrm{fus}}G(i)=\Delta_{\mathrm{fus}}H(i)\left(1-\frac{T}{T_{\mathrm{fus}}(i)}\right).$$

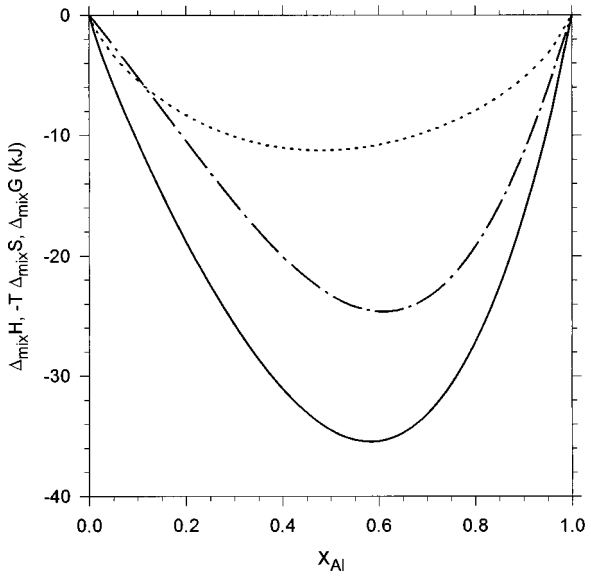

FIG. 14. Thermodynamic data of mixing in the liquid phase at $T=2000$ K obtained using the CVM model: Gibbs energy of mixing (solid line), enthalpy of mixing (dot-dashed line), and $-T\Delta_{\mathrm{mix}}S$, where $\Delta_{\mathrm{mix}}S$ is the entropy of mixing (dashed line).

TABLE VI. Summary of the thermodynamic data used in the phase diagram calculations.

bcc solid solution
$\Delta_{\mathrm{mix}}E=-13.1-5.1\xi_1+2.4\xi_2^1+9.6\xi_2^2+2.6\xi_3^1-3.3\xi_4^1$ (kJ/mol)
Liquid phase
$E_{\mathrm{dis}}=(1-\xi_1^2)(-22.6+10.4\xi_1)$ (kJ/mol)
$V_2^{(1)\mathrm{eff}}=1.5-2.2\xi_1$ (kJ/mol)
Intermetallic compounds
$AlNb_3\Delta_f G=-19.000-2.5\times10^{-3}$ T (kJ/mol of atoms)
$AlNb_2\Delta_f G=-24.900-2.4\times10^{-3}$ T (kJ/mol of atoms)
$Al_3Nb\Delta_f G=-41.500+2.2\times10^{-3}$ T (kJ/mol of atoms)
The reference state of the Gibbs energies of formation is bcc Nb and fcc Al
Lattice stability
$G_{\mathrm{Al}}^{\mathrm{bcc}}-G_{\mathrm{Al}}^{\mathrm{fcc}}=8.067$ kJ/mol[a]
$G_{\mathrm{Al}}^{\mathrm{bcc}}-G_{\mathrm{Al}}^{\mathrm{fcc}}=10.083-4.813$ T (kJ/mol)[b]

[a]This work.
[b]Reference 38.

(ii) The entropies of formation of the three intermetallic compounds are unknown. Since the interesting part of the phase diagram is in the temperature range 1500–2800 K, it is not realistic to suppose that the entropies of formation of these compounds referred to pure bcc Nb and fcc Al are negligible. Therefore we have adjusted the entropies of formation of the intermetallic compounds such a way that the temperatures of peritectic decomposition of $AlNb_3$ and $AlNb_2$ and the melting temperature of Al_3Nb are roughly reproduced. This also follows the standard CALPHAD approach.

(iii) The lattice stability of aluminum may be deduced from the total energy calculations for bcc Al and fcc Al. The value obtained in this work is $E_{\mathrm{Al}}^{\mathrm{bcc}}-E_{\mathrm{Al}}^{\mathrm{fcc}}=8.1$ kJ/mol. The difference of the Gibbs energies, a high temperature, has been taken equal to this last value, assuming that the entropy difference can be neglected. However, we have also tested the effect of using the CALPHAD value for the Al lattice stability: $G_{\mathrm{Al}}^{\mathrm{bcc}}-G_{\mathrm{Al}}^{\mathrm{fcc}}=10\,083.4-4.813$ T J/mol.

All the thermodynamic data used in these phase diagram calculations are reported in Table VI. In order to obtain the equilibrium phase diagram, we have minimized the grand potential Ω given by $\Omega=G-\mu^*\xi_1$, where μ^* is the effective chemical potential and ξ_1 the correlation function of the point cluster ($\xi_1=x_{\mathrm{Nb}}-x_{\mathrm{Al}}$). In the phases where the cluster variation method is used, the minimization is done using the natural iteration method developed by Kikuchi.[41] The equilibrium phase diagram between two phases I and II is computed using the same scheme as proposed by Kikuchi and Murray.[42]

Figure 15 presents the equilibrium phase diagram obtained using the lattice stability of Al obtained from the FP-LMTO calculations. The eutectic temperature where the liquid phase and the two compounds $AlNb_2$ and Al_3Nb are in equilibrium is found to be 100° lower than the experimental value. The only difference obtained by using the CALPHAD value of the aluminum lattice stability is an increase in the solubility of aluminum in bcc niobium (Fig. 16).

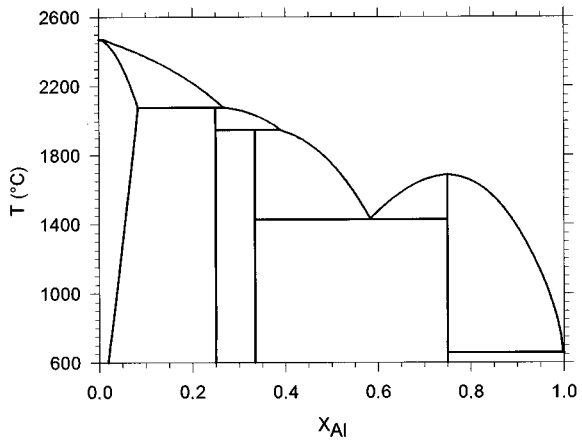

FIG. 15. Calculated Nb-Al phase diagram: the lattice stability of Al is deduced from the FP-LMTO calculations ($G_{Al}^{bcc} - G_{Al}^{fcc} = 8.1$ kJ/mol).

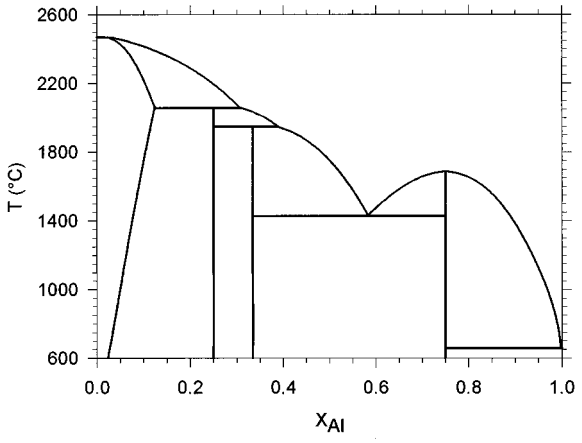

FIG. 16. Calculated Nb-Al phase diagram: the lattice stability of Al is deduced from CALPHAD compilations (Ref. 38) ($G_{Al}^{bcc} - G_{Al}^{fcc} = 10\,083.4 - 4.813\ T$ J mol^{-1})

VII. CONCLUSION

It has been shown that *ab initio* calculations in the Al-Nb binary alloy are in general in agreement with the available experimental information. The ground states are found to be $AlNb_3$ in the $A15$ structure, $AlNb_2$ in the σ structure, and Al_3Nb in the DO_{22} structure. It was also shown that the lattice relaxation and distortion play a crucial role in the stabilization of the latter phase. The enthalpies of formation of these compounds have been calculated, and the agreement with the available experimental data is quite satisfactory.

Our calculations indicate that the $B2$ phase is unstable in niobium-rich alloys and, therefore, cannot explain the experimental results obtained by Menon *et al.*[24] and Kohmoto *et al.*[43] for the presence of a $B2$ phase in quenched alloys containing ~ 20 at. % Al. The observations are, however, consistent with the high stability calculated for the ω phase in this region. It is possible for $B2$ to appear as a transient phase, as part of a transformation from bcc to metastable ω.

The enthalpies of formation of additional compounds based on fcc and bcc lattices have been deduced from total-energy full-potential LMTO calculations to derive the effective cluster interactions in bcc and fcc solid solutions. The bcc solid solution has been treated as a short-range-ordered phase. A modeling of the liquid phase has been proposed which takes into account of the disordering energies and the effective pair interactions obtained in the bcc and fcc phases.

The liquid-solid phase equilibrium has been calculated using three supplementary thermodynamic data: the entropies of formation of these compounds which have been adjusted from experimental phase diagram. The melting temperatures and the enthalpies of fusion of Al and Nb have been taken in recent compilations. Finally, the influence of the lattice stability on the aluminum solubility in bcc Nb has been discussed.

ACKNOWLEDGMENT

This work was supported by a computer grant of the ''Institut du Développement et des ressources en Informatique Scientifique'' (IDRIS).

[1] G. P. Srivastatva and D. Weaire, Adv. Phys. **36**, 463 (1987).
[2] R. Kikuchi, Phys. Rev. **81**, 988 (1951).
[3] K. Binder, in *Monte Carlo Methods in Statistical Physics*, edited by K. Binder, Springer Series on Topics in Current Physics Vol. 7 (Springer, Berlin, 1986).
[4] B. Velicky, S. Kirkpatrick, and H. Ehrenreich, Phys. Rev. **175**, 747 (1968).
[5] F. Ducastelle and F. Gautier, J. Phys. F **6**, 2039 (1976).
[6] L. Gyorffy and G. M. Stocks, Phys. Rev. Lett. **50**, 374 (1983).
[7] A. Gonis, X. G. Zhang, A. J. Freeman, P. Turchi, G. M. Stocks, and D. M. Nicholson, Phys. Rev. B **36**, 4630 (1987).
[8] A. Pasturel, J. Kudrnovsky, V. Drachal, and P. Weinberger, Phys. Rev. B **48**, 2704 (1993).
[9] J. W. Connolly and A. R. Williams, Phys. Rev. B **27**, 5169 (1983).
[10] S. H. Wei, L. G. Ferreira, and A. Zunger, Phys. Rev. **41**, 8240 (1990); Z. W. Lu, S. H. Wei, and A. Zunger, Phys. Rev. Lett. **66**, 1753 (1991).
[11] A. Pasturel, C. Colinet, D. Nguyen Manh, A. T. Paxton, and M. van Schilfgaarde, Phys. Rev. B **52**, 15 176 (1995).
[12] A. Pasturel, C. Colinet, A. T. Paxton, and M. van Schilfgaarde, J. Phys. Condens. Matter **4**, 945 (1992).
[13] A. Fernandez-Guillermet, V. Ozolins, G. Grimvall, and M. Körling, Phys. Rev. B **51**, 10 364 (1995).
[14] M. Asta, D. de Fontaine, and M. van Schilfgaarde, J. Mater. Res. **8**, 2554 (1993).
[15] M. Asta, D. de Fontaine, M. van Schilfgarade, M. Sluiter, and M. Methfessel, Phys. Rev. B **46**, 5055 (1992).
[16] Z. W. Lu, S. H. Wei, A. Zunger, S. Frota-Pessoa, and L. G. Ferreira, Phys. Rev. B **44**, 512 (1991).
[17] C. Wolverton and A. Zunger, Phys. Rev. B **50**, 10 548 (1994).
[18] M. Asta, R. McCormack, and D. de Fontaine, Phys. Rev. B **48**, 748 (1993).

[19] D. Nguyen-Manh, D. G. Pettifor, G. Shao, A. P. Miodownik, and A. Pasturel, Philos. Mag. A **74**, 1385 (1996).
[20] S. V. Meschel and O. J. Kleppa, J. Alloys Compd. **191**, 111 (1993).
[21] I. Shilo, H. F. Franzen, and R. A. Schiffman, J. Electrochem. Soc. **129**, 1608 (1982).
[22] *Binary Alloy Phase Diagrams*, 2nd ed., edited by T. B. Massalski (American Society for Metals, Metals Park, OH, 1990).
[23] *Pearson's Handbook of Crystallographic Data for Intermetallic Phases*, 2nd ed., edited by P. Villars and L. D. Calvert (American Society for Metals, Metals Park, OH, 1991).
[24] E. S. K. Menon, P. R. Subramanian, and D. M. Dimiduk, Scr. Metall. **27**, 265 (1992); Metall. Trans. A **27**, 1647 (1996).
[25] P. J. Craievch, M. Weinert, J. M. Sanchez, and R. E. Watson, Phys. Rev. Lett. **72**, 3076 (1994).
[26] M. Asta, A. Ormeci, J. M. Wills, and R. C. Albers, in *High-Temperature Ordered Intermetallic Alloys—VI*, edited by J. Horton *et al.*, MRS Symposia Preceedings No. 314 (Materials Research Society, Pittsburgh, 1995), p. 157.
[27] O. K. Andersen, Phys. Rev. B **12**, 3060 (1975).
[28] O. K. Andersen, in *Electronic Structure of Complex Systems*, edited by P. Phariseau and W. M. Temmerman (Plenum, New York, 1984), Vol. 5, p. 11.
[29] M. Methfessel, Phys. Rev. B **38**, 1537 (1988).
[30] A. T. Paxton, M. Methfessel, and H. M. Polatoglou, Phys. Rev. B **41**, 8127 (1990).
[31] U. von Barth and L. Hedin, J. Phys. C **5**, 1629 (1972).
[32] F. D. Murnaghan, Proc. Natl. Acad. Sci. USA **30**, 244 (1944).
[33] E. Passa, G. Shao, and P. Tsakiropoulos, Philos. Mag. A **75,** 587 (1997).
[34] N. Saunders, A. P. Miodownik, and A. T. Dinsdale, CALPHAD: Comput. Coupling Phase Diagrams Thermochem. **9,** 351 (1988).
[35] C. Kittel and H. Kroemer, *Thermal Physics*, 2nd ed. (Freeman, San Francisco, 1980).
[36] V. L. Moruzzi, J. F. Janak, and K. Schwark, Phys. Rev. B **37**, 790 (1988).
[37] A. Fernandez-Guillermet and W. Huang, Z. Metallkd. **79**, 88 (1988).
[38] A. Dinsdale, CALPHAD: Comput. Coupling Phase Diagrams Thermochem. **15,** 317 (1991).
[39] A. E. Carlsson, Phys. Rev. B **35**, 4858 (1987).
[40] M. Sluiter and P. E. A. Turchi, Phys. Rev. B **40**, 11 215 (1989).
[41] R. Kikuchi, J. Chem. Phys. **60**, 1071 (1974).
[42] R. Kikuchi and J. Murray, CALPHAD: Comput. Coupling Phase Diagrams Thermochem. **9,** 311 (1985).
[43] H. Kohmoto, J. Shyue, M. Aindow, and H. L. Fraser, Scr. Metall. **29**, 1271 (1993).